Hall conductivity of a two-dimensional graphite system

Yisong Zheng* and Tsuneya Ando
Institute for Solid State Physics, University of Tokyo, 5-1-5 Kashiwanoha, Kashiwa, Chiba 277-8581, Japan
(Received 13 September 2001; revised manuscript received 8 March 2002; published 18 June 2002)

Within a self-consistent Born approximation, the Hall conductivity of a two-dimensional graphite system in the presence of a magnetic field is studied by quantum transport theory. The Hall conductivity is calculated for short- and long-range scatterers. It is calculated analytically in the limit of strong magnetic fields and in the Boltzmann limit in weak magnetic fields. The numerical calculation shows that the Hall conductivity displays the quantum Hall effect when the Fermi energy is in low-lying Landau levels and the scattering is weak. When the Fermi energy becomes away from $\varepsilon=0$, it tends to the Boltzmann result.

DOI: 10.1103/PhysRevB.65.245420 PACS number(s): 73.50.−h, 72.10.−d, 72.80.Rj, 74.70.Wz

I. INTRODUCTION

Since the discovery of carbon nanotubes,[1] the transport property of a carbon network of nanometer scale has attracted much attention. There have been a lot of experimental works focusing on the transport measurement in various nanotube structures.[2–5] Meanwhile, the conductance of carbon nanotubes has been calculated using different approaches.[6–18] It is well known that a carbon nanotube consists of coaxially rolled two-dimensional (2D) graphite sheets. Therefore, the theoretical investigation on the transport property of the 2D graphite system is instructive for a comprehensive understanding of the transport property of the nanotubes.

In a previous work,[19] the density of states and the conductivity σ_{xx} were calculated by quantum transport theory, in which short- and long-range scatterers were taken into account. It was found that quantum theory provides results quite different from those of Boltzmann transport theory. In high magnetic fields, in particular, the conductivity exhibits a series of peaks, the values of which depend only on the natural constants and the Landau level index. In order to give a complete picture of the electronic transport property of this system, we elucidate the Hall conductivity in the present paper. As in the previous work, we will consider two cases in which the electron is scattered by short- and long-range scatterers and we will also employ a self-consistent Born approximation[20] (SCBA) in the quantum transport theory.

The paper is organized as follows: In Sec. II the effective Hamiltonian in the framework of the effective mass approximation is introduced and the eigenstates in the absence of scatterers are summarized. In Sec. III the Hall conductivity is calculated by using center migration theory. In Sec. IV numerical results are shown and discussed. In Appendixes A and B analytical demonstrations of the weak-magnetic-field limit and the Boltzmann limit are given. Last, there is a brief summary in Sec. V.

II. HAMILTONIAN

In a 2D graphite system, a unit cell contains two carbon atoms denoted as A and B. Two π bands having approximately a linear dispersion cross the Fermi level at K and K' points of the first Brillouin zone, whose wave vectors are given by $\mathbf{K}=(2\pi/a)(1/3,1/\sqrt{3})$ and $\mathbf{K}'=(2\pi/a)(2/3,0)$, with a being the lattice constant. The effective-mass Hamiltonian in the absence of scatterers in a magnetic field applied perpendicular to the system (the xy plane) is given by

$$\mathcal{H}_0=\frac{\gamma}{\hbar}\begin{pmatrix} 0 & \hat{\pi}_x-i\hat{\pi}_y & 0 & 0 \\ \hat{\pi}_x+i\hat{\pi}_y & 0 & 0 & 0 \\ 0 & 0 & 0 & \hat{\pi}_x+i\hat{\pi}_y \\ 0 & 0 & \hat{\pi}_x-i\hat{\pi}_y & 0 \end{pmatrix}, \tag{1}$$

where γ is a band parameter, $\hat{\boldsymbol{\pi}}=\hat{\mathbf{p}}+e\mathbf{A}/c$ with $\hat{\mathbf{p}}$ being the electron momentum operator, and $\mathbf{A}$ is the vector potential given by $\mathbf{A}=(0,Bx)$ in the Landau gauge. The corresponding Schrödinger equation

$$\mathcal{H}_0\mathbf{F}=\varepsilon\mathbf{F} \tag{2}$$

can be solved exactly.

In the absence of a magnetic field, the eigenfunction of $\mathcal{H}_0$ is given by

$$\mathbf{F}^K_{s\mathbf{k}}(\mathbf{r})=\frac{1}{\sqrt{2}L}\exp(i\mathbf{k}\cdot\mathbf{r})\begin{pmatrix} s \\ e^{i\varphi(\mathbf{k})} \\ 0 \\ 0, \end{pmatrix} \tag{3}$$

and

$$\mathbf{F}^{K'}_{s\mathbf{k}}(\mathbf{r})=\frac{1}{\sqrt{2}L}\exp(i\mathbf{k}\cdot\mathbf{r})\begin{pmatrix} 0 \\ 0 \\ e^{i\varphi(\mathbf{k})} \\ s \end{pmatrix}, \tag{4}$$

where L^2 is the area of the system, $\varphi(\mathbf{k})$ is the angle of the wave vector $\mathbf{k}$, and s denotes the bands ($s=+1$ for the conduction band and $s=-1$ for the valence band). The corresponding energy is given by

$$\varepsilon_{s\mathbf{k}}=s\gamma k, \tag{5}$$

with $k=|\mathbf{k}|$.

In the presence of a magnetic field, the eigenfunction $\mathbf{F}_{nk}^{j}$ is specified by a set of quantum numbers $\alpha=(j,n,k)$ where $j=K$ and K', the Landau level index $n=0,\pm1,\pm2,\ldots,$ and k is the electron wave vector in the y direction. The complete expression of eigenfunction is as follows:[21,22]

$$\mathbf{F}_{nk}^{K}(\mathbf{r})=\frac{C_n}{\sqrt{L}}\exp(-iky)\begin{pmatrix}\mathrm{sgn}(n)i^{|n|-1}\phi_{|n|-1}\\ i^{|n|}\phi_{|n|}\\ 0\\ 0\end{pmatrix} \tag{6}$$

and

$$\mathbf{F}_{nk}^{K'}(\mathbf{r})=\frac{C_n}{\sqrt{L}}\exp(-iky)\begin{pmatrix}0\\ 0\\ i^{|n|}\phi_{|n|}\\ \mathrm{sgn}(n)i^{|n|-1}\phi_{|n|-1}\end{pmatrix}, \tag{7}$$

with

$$C_n=\begin{cases}1 & (n=0),\\ 1/\sqrt{2} & (n\neq0),\end{cases} \tag{8}$$

$$\mathrm{sgn}(n)=\begin{cases}1 & (n>1),\\ 0 & (n=0),\\ -1 & (n<0),\end{cases} \tag{9}$$

and

$$\phi_{|n|}=\frac{1}{\sqrt{2^{|n|}|n|!\sqrt{\pi}l}}\exp\left[-\frac{1}{2}\left(\frac{x-l^2k}{l}\right)^2\right]H_{|n|}\left(\frac{x-l^2k}{l}\right), \tag{10}$$

where $l=\sqrt{c\hbar/eB}$ and $H_n(x)$ is the Hermite polynomial. The eigenenergy is dependent on the quantum number n only,

$$\varepsilon_n=\mathrm{sgn}(n)\hbar\omega\sqrt{|n|}, \tag{11}$$

$$\hbar\omega=\frac{\sqrt{2}\gamma}{l}. \tag{12}$$

It should be noted that $\hbar\omega$ has the dimension of energy but is not equivalent to the cyclotron frequency. According to Onsager's quantization scheme,[21] an energy spectrum similar to the above can be obtained semiclassically. However, the Landau level with $n=0$ is absent in the semiclassical spectrum, which indicates that the occurrence of such a level is totally a quantum effect.

We consider two different kinds of scatterers. First, the range of the scattering potential is smaller than the lattice constant of the 2D graphite. When such a short-range scatterer is present at a carbon A site $\mathbf{r}_i^A$, the effective Hamiltonian has been calculated as[11]

$$U_i^A(\mathbf{r})=\begin{pmatrix}1 & 0 & e^{i\phi_i^A} & 0\\ 0 & 0 & 0 & 0\\ e^{-i\phi_i^A} & 0 & 1 & 0\\ 0 & 0 & 0 & 0\end{pmatrix}u_i^A\delta(\mathbf{r}-\mathbf{r}_i^A), \tag{13}$$

with $\phi_i^A=(\mathbf{K}'-\mathbf{K})\cdot\mathbf{r}_i^A$ and u_i^A being the strength. Similarly, for a scatterer located at a carbon B site $\mathbf{r}_i^B$,

$$U_i^B(\mathbf{r})=\begin{pmatrix}0 & 0 & 0 & 0\\ 0 & 1 & 0 & e^{i\phi_i^B}\\ 0 & 0 & 0 & 0\\ 0 & e^{-i\phi_i^B} & 0 & 1\end{pmatrix}u_i^B\delta(\mathbf{r}-\mathbf{r}_i^B), \tag{14}$$

where $\phi_i^B=(\mathbf{K}'-\mathbf{K})\cdot\mathbf{r}_i^B$.

Next, the range is larger than the lattice constant but much smaller than the typical electron wavelength (which is infinite at $\varepsilon=0$). In this case matrix elements between K and K' points can be neglected and the potential is given by a diagonal matrix, i.e.,

$$U_i(\mathbf{r})=\begin{pmatrix}1 & 0 & 0 & 0\\ 0 & 1 & 0 & 0\\ 0 & 0 & 1 & 0\\ 0 & 0 & 0 & 1\end{pmatrix}u_i\delta(\mathbf{r}-\mathbf{r}_i), \tag{15}$$

where $\mathbf{r}_i$ is the impurity position. This type of scatterer is called a long-range one.

In the effective-mass approximation, the potential range of either scatterers (long or short range) is much smaller than the varying range of the wave functions which is scaled by the electron wave length. Therefore, we assume the same form of δ function for both long- and short-range potentials. This argument was examined in a previous work,[11] which showed that a Gaussian-type potential can be well approximated as a long-range potential as described by the above equation when the potential range is larger than the lattice constant; on the other hand, it can be regarded as a short-range potential when the range is smaller than half of the lattice constant. The classification of the scatterers into those of long and short range is made by the presence and absence of scattering between K and K' points.

Some actual point defects can be sorted into short- or long-range scatterers explicitly. For example, the fluorination of the graphite surface causes a kind of local π-electron defect, which is demonstrated to be a short-range scatterer by some calculations.[23] Adsorption induced by exposure of the graphite to ozone and ultraviolet radiation gives rise to a long-range scattering potential.[24] In addition, we can expect that a Coulomb impurity, the center of which is located in the substrate near the graphite sheet, will obviously be a long-range scatterer.

Some point defects have short- and long-range characteristics simultaneously. A recent experiment[25] reported that a boron atom in a boron-doped graphite surface brings about a notable correction on the electron density only in the range of one unit cell around it, which can be regarded as a short-

range scatterer. However, the boron atom slightly deforms the flatness of the graphite surface in a much larger range, which will cause a weak long-range scattering on the electron motion.[17]

The relaxation time in the absence of a magnetic field is defined as

$$\frac{1}{\tau}=\frac{2\pi}{\hbar}\sum_{j'=K,K'}\sum_{s'\mathbf{k}'}|\langle js\mathbf{k}|U|j's'\mathbf{k}'\rangle|^2\delta(\varepsilon_{s\mathbf{k}}-\varepsilon_{s'\mathbf{k}'}), \tag{16}$$

where U is the effective Hamiltonian for scatterers and $|js\mathbf{k}\rangle$ refers to the eigenfunction of $\mathcal{H}_0$ in the absence of magnetic field. In the case of short-range scatterers it is given by

$$\frac{1}{\tau}=\frac{1}{2}[n_i^A\langle(u_i^A)^2\rangle+n_i^B\langle(u_i^B)^2\rangle]\frac{|\varepsilon|}{\hbar\gamma^2}, \tag{17}$$

where n_i^A and n_i^B are the concentration of scatterers in a unit area and $\langle\cdots\rangle$ means the average. The relaxation time for long-range scatterers is given by

$$\frac{1}{\tau}=n_i\langle(u_i)^2\rangle\frac{|\varepsilon|}{2\hbar\gamma^2}. \tag{18}$$

When we assume $u^2=\langle(u_i^A)^2\rangle=\langle(u_i^B)^2\rangle=\langle(u_i)^2\rangle$ and $n_i=n_i^A+n_i^B$ and $n_i^A=n_i^B$, the relaxation time becomes the same between short- and long-range cases and

$$\frac{1}{\tau}=\frac{2\pi|\varepsilon|}{\hbar A}, \tag{19}$$

where we have introduced a dimensionless parameter to characterize the scattering strength given by

$$A=\frac{4\pi\gamma^2}{n_iu^2}. \tag{20}$$

With the use of the Boltzmann transport equation, the transport relaxation time is given by

$$\frac{1}{\tau_{\rm tr}}=\frac{2\pi}{\hbar}\sum_{j'=K,K'}\sum_{s'\mathbf{k}'}|\langle js\mathbf{k}|U|j's'\mathbf{k}'\rangle|^2(1-\cos\theta)\times\delta(\varepsilon_{s\mathbf{k}}-\varepsilon_{s'\mathbf{k}'}), \tag{21}$$

where $\cos\theta=\mathbf{k}\cdot\mathbf{k}'/k^2$. In the case of short-range scatterers, $\tau_{\rm tr}=\tau$, while $\tau_{\rm tr}=2\tau$ in the case of long-range scatterers because of the absence of backward scattering. Consider the case $\varepsilon>0$ first. The classical equation of motion is given by

$$\hbar\frac{d\mathbf{k}}{dt}=-\frac{e}{c}\mathbf{v}\times\mathbf{B}, \tag{22}$$

in the presence of a magnetic field $\mathbf{B}$, where $\mathbf{v}$ is the velocity. This gives the cyclotron frequency $\omega_c=eBv^2/c\varepsilon$, where v is the electron velocity given by $v=|\mathbf{v}|=\gamma/\hbar$. Note that ω_c diverges at $\varepsilon=0$. The conductivity tensor $\sigma_{\mu\nu}$ is calculated as

$$\sigma_{xx}=\sigma_{yy}=\frac{\sigma_0}{1+(\omega_c\tau_{\rm tr})^2},\quad \sigma_{xy}=-\sigma_{yx}=-\frac{\omega_c\tau_{\rm tr}\sigma_0}{1+(\omega_c\tau_{\rm tr})^2}, \tag{23}$$

with

$$\sigma_0=\frac{e^2}{\pi^2\hbar}\frac{A}{4}\frac{\tau_{\rm tr}}{\tau}. \tag{24}$$

In weak magnetic fields $\omega_c\tau_{\rm tr}\ll 1$, we have the relation

$$\sigma_{xy}=-\omega_c\tau_{\rm tr}\sigma_0, \tag{25}$$

and in high magnetic fields $\omega_c\tau_{\rm tr}\gg 1$,

$$\Delta\sigma_{xy}=\sigma_{xy}+\frac{n_eec}{B}=-\frac{1}{\omega_c\tau_{\rm tr}}\sigma_{xx}, \tag{26}$$

where n_e is the electron density measured from $\varepsilon=0$. In a weak magnetic field, the Hall conductivity diverges as ε^{-2} at $\varepsilon=0$, because σ_0 is independent of energy and both $\omega_c\propto\varepsilon^{-1}$ and $\tau_{\rm tr}\propto\varepsilon^{-1}$ diverge. The above discussion holds even for $\varepsilon<0$, if we set

$$\omega_c=\frac{eBv^2}{c\varepsilon}=\mathrm{sgn}(\varepsilon)\frac{eBv^2}{c|\varepsilon|}. \tag{27}$$

If we put $\varepsilon=\varepsilon_n$, we have $\hbar\omega_c=\mathrm{sgn}(n)(\hbar\omega/2\sqrt{|n|})$.

III. HALL CONDUCTIVITY

The Kubo formula concerning the conductivity as a linear response function to an external field is written as[26]

$$\sigma_{\mu\nu}=\int_0^\infty dt\int_0^\beta d\lambda e^{-st}\langle j_\nu(-i\hbar\lambda)j_\mu(t)\rangle\quad(s\to+0), \tag{28}$$

where j_μ is the μth component of the current $-e\dot{x}_\mu$ with $\dot{x}$ the velocity and $-e$ the electronic charge, $j_\mu(t)$ the Heisenberg representation of the current operator j_μ, $\langle\cdots\rangle$ means the average over the canonical ensemble, and $\beta=1/k_BT$ with T being the temperature.

In the presence of a magnetic field perpendicular to the 2D surface, the electron coordinate operators x and y are decomposed into two parts as follows:[27]

$$x=\xi+X,\quad y=\eta+Y, \tag{29}$$

where X and Y are called the guiding center coordinates, and ξ and η are called the relative coordinates of the cyclotron motion, defined by

$$\xi=\frac{l^2\pi_y}{\hbar},\quad \eta=-\frac{l^2\pi_x}{\hbar}. \tag{30}$$

In a magnetic field, (X,Y) and (ξ,η) constitute a set of canonical variables for the dynamics of the electron. Substituting Eq. (29) into the original Kubo formula, Eq. (28), a set of new formulas for the Hall conductivity in the framework of so-called center migration theory can be obtained, which reads[27–29]

$$\sigma_{xy} = -\frac{n_e e c}{B} + \Delta\sigma_{xy} \tag{31}$$

and

$$\Delta\sigma_{xy} = \frac{e^2\hbar}{i\pi L^2}\int_0^\infty f(\varepsilon)d\varepsilon \times \left\langle \mathrm{Tr}\dot{X}\left(\frac{\partial}{\partial\varepsilon}\mathrm{Re}G(\varepsilon+i0)\right)\dot{Y}\,\mathrm{Im}G(\varepsilon+i0) - (\dot{X}\leftrightarrow\dot{Y})\right\rangle, \tag{32}$$

where $f(\varepsilon)$ is the Fermi distribution function and the Green function $G(\varepsilon)$ is defined as

$$G(\varepsilon) = \frac{1}{\varepsilon - \mathcal{H}} \tag{33}$$

and

$$\begin{pmatrix} \dot{X} \\ \dot{Y} \end{pmatrix} = \frac{l}{\hbar}\begin{pmatrix} l\dfrac{\partial}{\partial y} \\ -l\dfrac{\partial}{\partial x} \end{pmatrix} U(\mathbf{r}). \tag{34}$$

The center migration theory is equivalent to the original Kubo formula when dealing with the conductivity in a magnetic field.[29] It has an advantage in the study of the high-field transport because it gives clear physical pictures in that the electron transport may be viewed as a diffusionlike process of the electron orbital which has a localized character.[27]

The π bands of 2D graphite where the Fermi level lies is symmetric about $\varepsilon = 0$ in the effective-mass approximation. If being combined with the usual fact that the Hall conductivity vanishes when a band is completely occupied, this leads to the reasonable assumption that the Hall conductivity vanishes in undoped 2D graphite with the Fermi level at $\varepsilon = 0$. In the above expressions, therefore, the lower limit of the integral has been chosen to be $\varepsilon = 0$ and the electron density n_e should also be regarded as the electron number above $\varepsilon = 0$ ($n_e < 0$ for $\varepsilon < 0$).

With a little trick Eq. (32) can be formally changed into

$$\Delta\sigma_{xy} = -\frac{e^2\hbar}{4\pi L^2}\int f(\varepsilon)d\varepsilon \lim_{\varepsilon'\to\varepsilon}\frac{\partial}{\partial\varepsilon'}\langle \mathrm{Tr}\dot{X}[G(\varepsilon'+i0) + G(\varepsilon'-i0)]\dot{Y}[G(\varepsilon+i0) - G(\varepsilon-i0)] - (\dot{X}\leftrightarrow\dot{Y})\rangle. \tag{35}$$

From the above equation it can be seen that it is essential to treat the quantity

$$J = \langle[\mathrm{Tr}\dot{X}G(\varepsilon')\dot{Y}G(\varepsilon)]\rangle, \tag{36}$$

which is equivalent to the diagrams shown in Fig. 1 in the SCBA. Now, $\Delta\sigma_{xy}$ is divided into two parts named $\Delta\sigma_{xy}^{(1)}$ and $\Delta\sigma_{xy}^{(2)}$ corresponding to the diagrams shown by Figs. 1(a) and 1(b). In Fig. 1 all Green functions refer to the average ones over all configurations of scatterers. In addition to

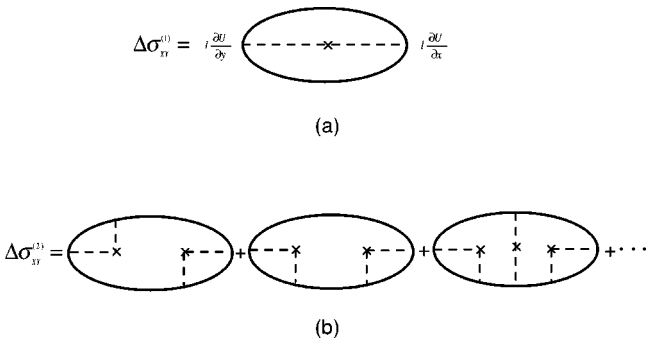

FIG. 1. Diagrams of $\Delta\sigma_{xy}$ in the self-consistent Born approximation (SCBA). (a) $\Delta\sigma_{xy}^{(1)}$. (b) Some examples of $\Delta\sigma_{xy}^{(2)}$.

the so-called proper vertex part a new quantity $\xi_{\alpha\alpha'}(\varepsilon,\varepsilon')$ has been introduced in Fig. 1(b), which may be called the ξ part.[30] It is obtained graphically from a self-energy diagram by replacing one of matrix elements of the potential $U(\mathbf{r})$ by the corresponding $l\partial U(\mathbf{r})/\partial y$ or $l\partial U(\mathbf{r})/\partial x$ as shown more clearly in Fig. 2. It can be justified that $\Delta\sigma_{xy}^{(1)}$ vanishes identically in the SCBA and only $\Delta\sigma_{xy}^{(2)}$ has a contribution to the Hall conductivity.

A. Case of short-range scatterers

In the case of short-range scatterers, the averaged Green function and self-energy over scatterer configurations are diagonal. They are

$$\langle G_{\alpha\alpha'}(\varepsilon)\rangle = \delta_{\alpha\alpha'}G_n(\varepsilon), \qquad \Sigma_{\alpha\alpha'}(\varepsilon) = \delta_{\alpha\alpha'}\Sigma(\varepsilon). \tag{37}$$

In the SCBA the self-energy $\Sigma(\varepsilon)$ can be determined by the self-consistency equation

$$\Sigma(\varepsilon) = \frac{(\hbar\omega)^2}{2A}\sum_{n=-N_c}^{N_c}\frac{1}{\varepsilon - \varepsilon_n - \Sigma(\varepsilon)}. \tag{38}$$

In the above equation, a cutoff number N_c is necessary to truncate the summation because the infinite summation in the right side leads to a logarithmic divergence. The cutoff N_c should be chosen such that the corresponding cutoff energy $\epsilon_c = \sqrt{N_c}\hbar\omega$ should be of the order of the bandwidth.[15]

The ξ part can be calculated as follows:

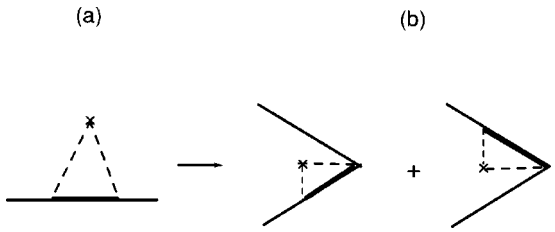

FIG. 2. The self-energy and corresponding ξ part in the SCBA.

$$\xi^{y}_{\alpha\alpha'}(\varepsilon,\varepsilon') = -\delta_{j,j'}\delta_{k,k'}\frac{C_n C_{n'}}{\sqrt{2}}\{[\sqrt{|n|} + \mathrm{sgn}(n)\mathrm{sgn}(n')\sqrt{|n'|}]\delta_{|n'|,|n|-1} - [\sqrt{|n'|} + \mathrm{sgn}(n)\mathrm{sgn}(n')\sqrt{|n|}]\delta_{|n|,|n'|-1}\} \times [\Sigma(\varepsilon)-\Sigma(\varepsilon')], \tag{39}$$

$$\xi^{x}_{\alpha\alpha'}(\varepsilon,\varepsilon') = -i\delta_{j,j'}\delta_{k,k'}\frac{C_n C_{n'}}{\sqrt{2}}\{[\sqrt{|n|} + \mathrm{sgn}(n)\mathrm{sgn}(n')\sqrt{|n'|}]\delta_{|n'|,|n|-1} + [\sqrt{|n'|} + \mathrm{sgn}(n)\mathrm{sgn}(n')\sqrt{|n|}]\delta_{|n|,|n'|-1}\} \times [\Sigma(\varepsilon)-\Sigma(\varepsilon')]. \tag{40}$$

From Eqs. (39) and (40) it can be readily found that the following conditions are satisfied:

$$\xi^{y}_{\alpha'\alpha}(\varepsilon',\varepsilon) = \xi^{y}_{\alpha\alpha'}(\varepsilon,\varepsilon'),$$

$$\xi^{x}_{\alpha'\alpha}(\varepsilon',\varepsilon) = -\xi^{x}_{\alpha\alpha'}(\varepsilon,\varepsilon'). \tag{41}$$

All diagrams involving the vertex parts in Fig. 1(b) include such a factor as $\xi^{y}_{\alpha_1\alpha_1'}(\varepsilon,\varepsilon')\langle U_{\alpha_1'\alpha_2'}U_{\alpha_2\alpha_1}\rangle$, which results in a product of two delta functions $\delta_{|n_1'|,|n_1|\pm 1}\delta_{|n_1'|,|n_1|}$. Because of their incompatibility, the vertex corrections vanish in the case of short-range scatterers. By using Eqs. (39)–(41), $\Delta\sigma_{xy}$ in the SCBA can be obtained for the case of short-range scatterers as

$$\Delta\sigma_{xy} = \int d\varepsilon\left(-\frac{\partial f}{\partial\varepsilon}\right)\Delta\sigma_{xy}(\varepsilon), \tag{42}$$

with

$$\Delta\sigma_{xy}(\varepsilon) = \frac{e^2}{\pi^2\hbar}\frac{2(\mathrm{Im}\Sigma)^2}{(\hbar\omega)^2}\mathrm{Im}\sum_{n\geqslant 0}[2|\varepsilon-\Sigma(\varepsilon)|^2 + (2n+1)(\hbar\omega)^2]g_n(\varepsilon+i0)g_{n+1}(\varepsilon-i0), \tag{43}$$

where

$$g_n(\varepsilon) = \frac{1}{2}(G_n+G_{-n}) = \frac{\varepsilon-\Sigma(\varepsilon)}{[\varepsilon-\Sigma(\varepsilon)]^2-|n|(\hbar\omega)^2}. \tag{44}$$

We consider a particular situation as the magnetic field is very strong, the scattering is relatively weak, and the energy ε is in the vicinity of the Nth Landau level, i.e., $\varepsilon\sim\varepsilon_N$, which is called hereafter the strong magnetic field limit. Under this situation the self-energy can be solved by retaining only a term with $n=N$ in the summation of the self-consistency equation. In this case the density of states is calculated as

$$D(\varepsilon) = -\frac{A\mathrm{Im}\Sigma}{\pi^2\gamma^2} = \frac{2}{2\pi l^2}\frac{2}{\pi\Gamma}\left[1-\left(\frac{\varepsilon-\varepsilon_N}{\Gamma}\right)^2\right]^{1/2}, \tag{45}$$

with

$$\Gamma = \frac{\sqrt{2}\hbar\omega}{\sqrt{A}}. \tag{46}$$

Accordingly, an approximate expression of $\Delta\sigma_{xy}(\varepsilon)$ correct up to the order $\Gamma/\hbar\omega$ becomes

$$\Delta\sigma_{xy}(\varepsilon) = \frac{e^2}{\pi^2\hbar}\mathrm{sgn}(N)\frac{4|N|^{3/2}\Gamma}{\hbar\omega}\left[1-\left(\frac{\varepsilon-\varepsilon_N}{\Gamma}\right)^2\right]^{3/2}, \tag{47}$$

which vanishes for the Landau level $N=0$. The corresponding expression of conductivity σ_{xx} is given by[19]

$$\sigma_{xx}(\varepsilon) = \frac{e^2}{\pi^2\hbar}(2|N|+\delta_{N0})\left[1-\left(\frac{\varepsilon-\varepsilon_N}{\Gamma}\right)^2\right]. \tag{48}$$

The above shows that there is the relation between σ_{xx} and $\Delta\sigma_{xy}$ as

$$\Delta\sigma_{xy}(\varepsilon) = -\frac{2\,\mathrm{Im}\,\Sigma}{\hbar\omega_c}\sigma_{xx}(\varepsilon), \tag{49}$$

with ω_c given by Eq. (27) at $\varepsilon=\varepsilon_N$. This is equivalent with Eq. (26) when $\hbar/\tau_{\mathrm{tr}}=\hbar/\tau$ is replaced by $-2\mathrm{Im}\Sigma(\varepsilon)$.

In Appendix A, the Hall conductivity σ_{xy} is demonstrated to vanish identically in the limit of zero magnetic field. It is quite tedious to obtain an explicit expression of σ_{xy} in the weak-field limit and therefore we shall consider only the Boltzmann limit where the broadening $\hbar/\tau$ is much smaller than energy $|\varepsilon|$. Explicit calculations are performed in Appendix B and give

$$\sigma_{xy} = -\omega_c\tau\sigma_0, \tag{50}$$

in perfect agreement with the result of Boltzmann transport theory.

B. Case of long-range scatterers

In the case of long-range scatterers, K and K' are decoupled and have the same contributions to the Hall conductivity. Therefore, at first we shall focus on the K point only to deal with the Hall conductivity and then multiply the final results by a factor of 2. Unlike the case of short-range scatterers, the averaged Green function and the self-energy are not diagonal with respect to the Landau level index and have off-diagonal elements between $+n$ and $-n$. They are expressed as

$$\Sigma_{\alpha\alpha'}(\varepsilon) = \delta_{\alpha\alpha'}\Sigma^{d}(\varepsilon) + \delta_{\alpha-\alpha'}\Sigma^{o}(\varepsilon),$$

$$\langle G_{\alpha\alpha'}(\varepsilon)\rangle = \delta_{\alpha\alpha'}G^{d}_{n}(\varepsilon) + \delta_{\alpha-\alpha'}G^{o}_{n}(\varepsilon), \tag{51}$$

where $\pm\alpha=(\pm n,k)$. By defining $\Sigma^{\pm}=\Sigma^{d}\pm\Sigma^{o}$, the self-consistency equation to determine the self-energy is given by

$$\Sigma^+ = \frac{(\hbar\omega)^2}{A}\sum_{n=0}^{N_c}\frac{\varepsilon-\Sigma^-}{(\varepsilon-\Sigma^+)(\varepsilon-\Sigma^-)-\varepsilon_n^2},$$

$$\Sigma^- = \frac{(\hbar\omega)^2}{A}\sum_{n=1}^{N_c}\frac{\varepsilon-\Sigma^+}{(\varepsilon-\Sigma^+)(\varepsilon-\Sigma^-)-\varepsilon_n^2}. \quad (52)$$

The ξ parts take the following forms:

$$\xi^y_{\alpha\alpha'}(\varepsilon,\varepsilon') = \xi^{y+}_{\alpha\alpha'}(\varepsilon,\varepsilon') + \xi^{y-}_{\alpha\alpha'}(\varepsilon,\varepsilon'), \quad (53)$$

with

$$\begin{aligned}\xi^{y+}_{\alpha\alpha'}(\varepsilon,\varepsilon') &= \delta_{kk'}\frac{C_nC_{n'}}{\sqrt{2}}\{\sqrt{|n|}\,\mathrm{sgn}(n)\mathrm{sgn}(n')[\Sigma^-(\varepsilon)-\Sigma^-(\varepsilon')] \\ &\quad -\mathrm{sgn}(n')[Z(\varepsilon)-Z(\varepsilon')] \\ &\quad +\sqrt{|n'|}[\Sigma^+(\varepsilon)-\Sigma^+(\varepsilon')]\}\delta_{|n'|,|n|+1} \quad (54)\end{aligned}$$

and

$$\begin{aligned}\xi^{y-}_{\alpha\alpha'}(\varepsilon,\varepsilon') &= -\delta_{kk'}\frac{C_nC_{n'}}{\sqrt{2}}\{\sqrt{|n'|}\,\mathrm{sgn}(n)\mathrm{sgn}(n')[\Sigma^-(\varepsilon)-\Sigma^-(\varepsilon')] \\ &\quad -\mathrm{sgn}(n)[Z(\varepsilon)-Z(\varepsilon')] \\ &\quad +\sqrt{|n|}[\Sigma^+(\varepsilon)-\Sigma^+(\varepsilon')]\}\delta_{|n|,|n'|+1}, \quad (55)\end{aligned}$$

where a new quantity

$$Z(\varepsilon) = (\hbar\omega)^{-1}\Sigma^-(\varepsilon)[\varepsilon-\Sigma^-(\varepsilon)] \quad (56)$$

has been defined. Further, $\xi^x_{\alpha\alpha'}(\varepsilon,\varepsilon')$ is associated with $\xi^y_{\alpha\alpha'}(\varepsilon,\varepsilon')$ through the relation

$$\xi^x_{\alpha\alpha'}(\varepsilon,\varepsilon') = \xi^{x+}_{\alpha\alpha'}(\varepsilon,\varepsilon') + \xi^{x-}_{\alpha\alpha'}(\varepsilon,\varepsilon'), \quad (57)$$

$$\xi^{x\pm}_{\alpha\alpha'}(\varepsilon,\varepsilon') = \mp i\,\xi^{y\pm}_{\alpha\alpha'}(\varepsilon,\varepsilon'). \quad (58)$$

With the above results the Hall conductivity can be derived by dealing with the diagrams illustrated by Fig. 1(b). Unlike in the case of short-range scatterers, the vertex corrections have contributions to the Hall conductivity. Therefore, all diagrams in Fig. 1(b) have to be taken into account. After a tedious derivation an expression of $\Delta\sigma_{xy}$ is obtained as follows:

$$\Delta\sigma_{xy}(\varepsilon) = \sigma_a + \sigma_b, \quad (59)$$

with

$$\begin{aligned}\sigma_a &= \frac{e^2}{\pi^2\hbar}\frac{2A}{(\hbar\omega)^4}\{\mathrm{Re}\Sigma^+\mathrm{Im}\Sigma^-[(\mathrm{Im}\Sigma^+)^2+(\mathrm{Im}\Sigma^-)^2] \\ &\quad +\varepsilon[(\mathrm{Im}\Sigma^+)^3-(\mathrm{Im}\Sigma^-)^3] \\ &\quad -\mathrm{Re}\Sigma^-\mathrm{Im}\Sigma^+[(\mathrm{Im}\Sigma^+)^2+(\mathrm{Im}\Sigma^-)^2]\} \quad (60)\end{aligned}$$

and

$$\sigma_b = \frac{e^2}{\pi^2\hbar}\mathrm{Im}\left[\frac{s(\varepsilon)}{1-\varphi(\varepsilon-i0,\varepsilon+i0)}\right], \quad (61)$$

where

$$\varphi(\varepsilon,\varepsilon') = \frac{(\hbar\omega)^2}{A}\sum_{n=0}^{\infty} g_n^+(\varepsilon)g_{n+1}^-(\varepsilon'), \quad (62)$$

$$g_n^\pm(\varepsilon) = \frac{\varepsilon-\Sigma^\mp(\varepsilon)}{[\varepsilon-\Sigma^+(\varepsilon)][\varepsilon-\Sigma^-(\varepsilon)]-\varepsilon_n^2} \quad (63)$$

and

$$\begin{aligned}s(\varepsilon) &= -\frac{2A}{(\hbar\omega)^4}[\Sigma^-*\mathrm{Im}\Sigma^- + \varepsilon\mathrm{Im}\Sigma^+ \\ &\quad -\Sigma^+*\mathrm{Im}\Sigma^+ - \mathrm{Im}(\Sigma^+\Sigma^-)]^2. \quad (64)\end{aligned}$$

It should be noted that the contribution of K' has been added.

In the strong-magnetic-field limit, when the energy is close to the Nth Landau level, i.e., $\varepsilon\sim\varepsilon_N$, approximate expressions can be obtained. We have

$$D(\varepsilon) = \frac{1}{2\pi l^2}\frac{2}{\pi\Gamma_N}\left[1-\left(\frac{\varepsilon-\varepsilon_N}{\Gamma_N}\right)^2\right]^{1/2} \quad (65)$$

and

$$\Delta\sigma_{xy}(\varepsilon) = \frac{e^2}{\pi^2\hbar}\mathrm{sgn}(N)\frac{|N|^{3/2}\Gamma_N}{\hbar\omega}\left[1-\left(\frac{\varepsilon-\varepsilon_N}{\Gamma_N}\right)^2\right]^{3/2}, \quad (66)$$

with $\Gamma_N=\Gamma$ for $N\neq 0$ and $\Gamma_0=\sqrt{2}\Gamma$. The above vanishes for $N=0$. The diagonal conductivity has been calculated as[19]

$$\sigma_{xx}(\varepsilon) = \frac{e^2}{\pi^2\hbar}(|N|+\delta_{N0})\left[1-\left(\frac{\varepsilon-\varepsilon_N}{\Gamma_N}\right)^2\right]. \quad (67)$$

The above shows that there is the relation between σ_{xx} and $\Delta\sigma_{xy}$ as

$$\Delta\sigma_{xy}(\varepsilon) = -\frac{\mathrm{Im}\Sigma}{\hbar\omega_c}\sigma_{xx}(\varepsilon), \quad (68)$$

with ω_c given by Eq. (27) at $\varepsilon=\varepsilon_N$. The deviation $\Delta\sigma_{xy}$ is proportional to σ_{xx} and $\mathrm{Im}\Sigma$, but the coefficient is a half of that in the short-range case. This difference corresponds to the relation $\tau_{\mathrm{tr}}=2\tau$. Because the diagonal conductivity is smaller by a factor of 2 for $N\neq 0$, the peak value of $\Delta\sigma_{xy}$ becomes smaller by a factor of 4 than that in the case of short-range scatterers.

In the Boltzmann limit in weak magnetic fields, on the other hand, we have

$$\sigma_{xy} = -\omega_c\tau_{\mathrm{tr}}\sigma_0, \quad (69)$$

in perfect agreement with the result of the Boltzmann transport theory. The above is proportional to τ_{tr}^2 and therefore, for the same value of the effective scattering parameter A, $|\sigma_{xy}|$ is 4 times as large as that in the case of short-range scatterers.

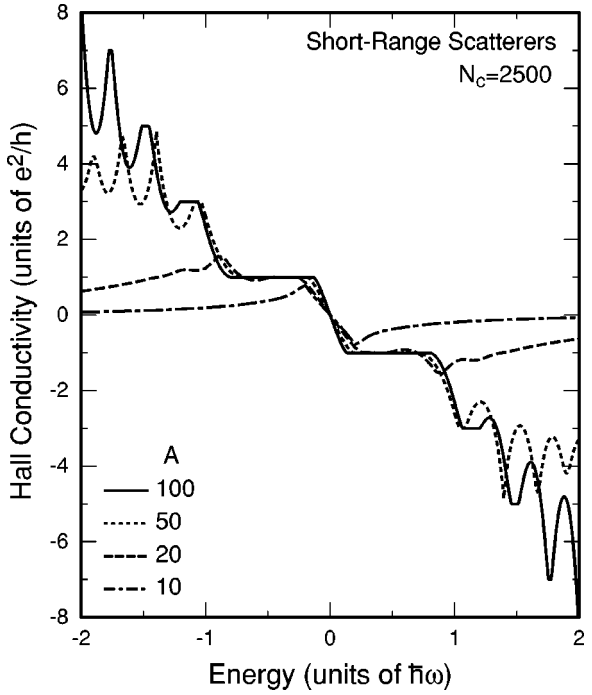

FIG. 3. The Hall conductivity σ_{xy} as a function of energy for $A=100$, 50, 20, and 10 for the case of short-range scatterers.

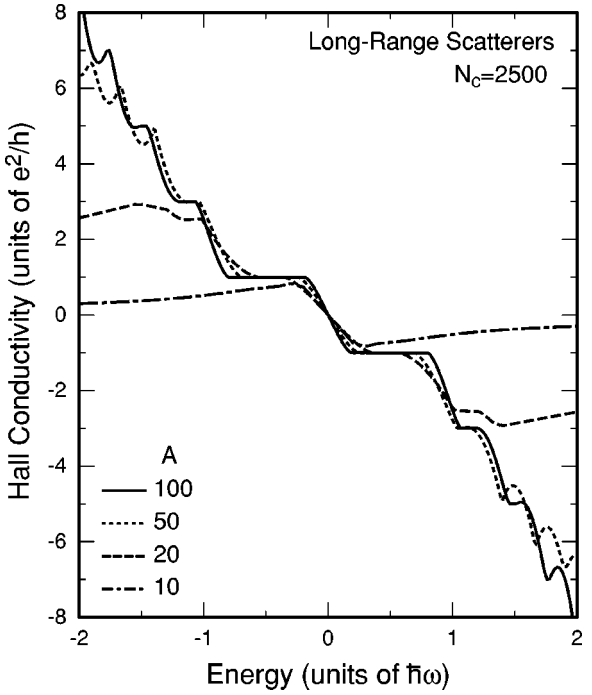

FIG. 4. The Hall conductivity σ_{xy} as a function of energy for $A=100$, 50, 20, and 10 for the case of long-range scatterers.

IV. NUMERICAL RESULTS AND DISCUSSION

The self-consistency equations to determine the self-energy, Eqs. (38) and (52), can be solved numerically by iteration method, and the resulting self-energy is used for calculations of the Hall conductivity. In Fig. 3 the calculated Hall conductivity is shown as a function of the Fermi energy ε for several typical scattering strength in the case of short-range scatterers. Following the previous work,[2] the Landau level index corresponding to the cutoff energy is chosen as $N_c=2500$. When the scattering is relatively weak ($A=100$ and 50), the Hall conductivity has a steplike structure as a function of ε at the region of low-lying Landau levels, which reflects the quantum Hall effect. The positions of plateau occur at the forbidden regions of the density of the states between Landau levels.[19] On the other hand, when the Fermi energy is at regions corresponding to higher Landau levels, the spacing between the adjacent Landau levels becomes narrow and therefore scattering effects become more dominant. As a result, the Hall conductivity displays peaks instead of a plateau in these regions. There is no Hall plateau in the cases of sufficiently strong scattering ($A=20$ and 10) due to the strong overlap of the electron density of states.[19]

Figure 4 shows the numerical result for the case of long-range scatterers. The Hall conductivity is a little larger than the corresponding value of the case of short-range scatterers except when the Fermi level lies in a gap between neighboring Landau levels and it is quantized into an integer multiple of e^2/h. This is due to the lack of the backscattering, leading to a reduction of $\Delta\sigma_{xy}$ by a factor of 4 in the case of the long-range scatterers, mentioned in the previous section.

In Figs. 5 and 6 the calculated Hall conductivity corresponding to the short- and long-range scatterers, respectively, is plotted in a larger energy range. The corresponding results of the Boltzmann transport theory are also shown. From these two figures it can be found that when the energy is far away from the vicinity of zero, the Hall conductivity in the SCBA agrees with the corresponding Boltzmann result very

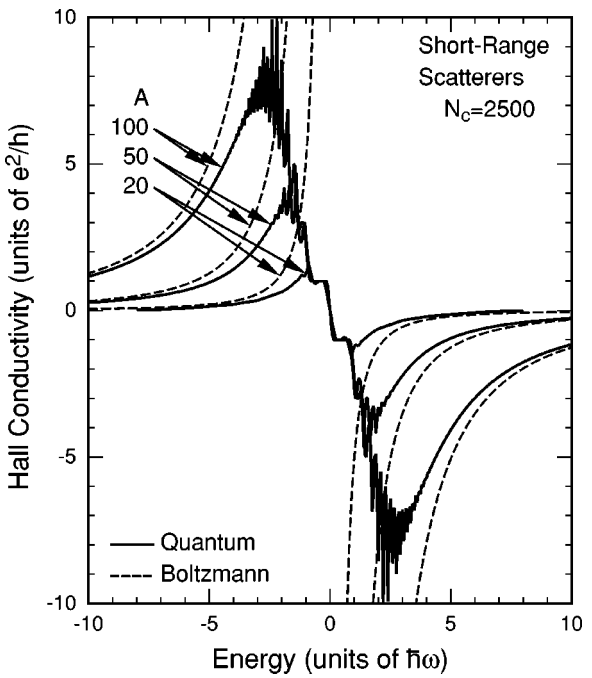

FIG. 5. The Hall conductivity σ_{xy} as a function of energy for $A=100$, 50, and 20 for the short-range scatterers. The corresponding results of Boltzmann transport theory are shown by dashed lines.

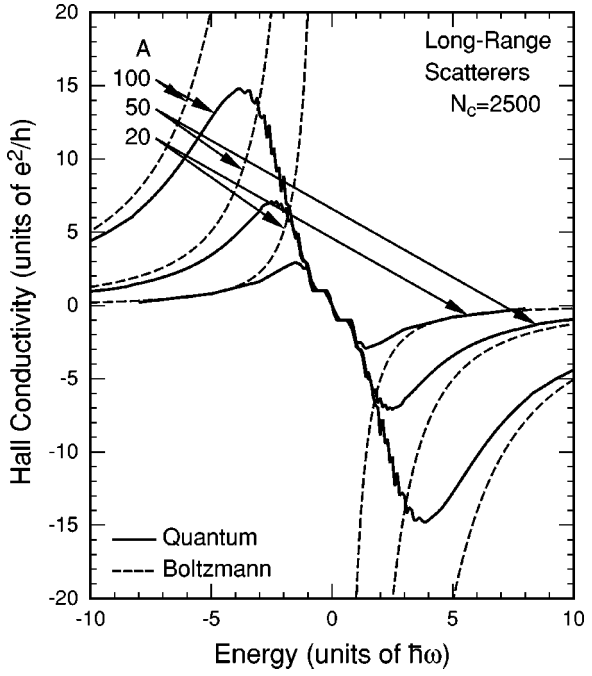

FIG. 6. The Hall conductivity σ_{xy} as a function of energy for $A=100$, 50, and 20 for long-range scatterers. The corresponding results of Boltzmann transport theory are shown by dashed lines.

well, especially when the scattering strength is very weak. On the contrary, when the energy is close to zero, the results in the SCBA depart from the Boltzmann results, which implies that in this region semiclassical Boltzmann theory is not adequate to describe the Hall conductivity of the 2D graphite system. By comparing Fig. 5 with Fig. 6, it can be found that the Hall conductivity in the case of long-range scatterers is always larger than the corresponding value in the case of short-range scatterers.

A 2D system with parabolic band structure always exhibits a sinusoidal oscillation in the diagonal and Hall conductivities as Fermi energy increases, accompanying the main trends to the Boltzmann limits.[30,31] On the contrary, the oscillating characteristic disappears rapidly in the conductivities in the present 2D graphite system with the increase of the Fermi energy as shown in Figs. 5 and 6. This is the direct consequence of the linear and zero-gap band structure described by Eq. (5) in the graphite sheet. In fact, the space between the adjacent Landau levels with large indexes becomes very small. Thus the scattering effect suppresses oscillation of the density of states in this range, which results in an agreement of the quantum conductivities with the Boltzmann results when the Fermi energy is far away from the low-lying Landau levels.

In usual single-wall nanotubes the quantum coherence of the electron wave around the circumference determines whether they become metallic or semiconducting.[18] The situation is expected to be same in multiwall nanotubes. In multiwall nanotubes it is believed that most of the current is carried by a few outermost metallic nanotubes. Oscillations of the conductance ascribed to the Altshuler-Aronov-Spivak type[32] and those ascribed to the Aharonov-Bohm effect on the band structure[33] were observed in thick multiwall nanotubes in the presence of a magnetic field parallel to the axis.[34,35] In these experiments the phase coherence length was estimated to be only of the order of the circumference even at very low temperatures.[34,35] This shows that coherence along the circumference may not be so perfect in thick multiwall nanotubes.

When the phase coherence length is smaller than the circumference, the transport may approximately be described by local conductivities σ_{xx} and σ_{xy} in a 2D graphite system. In such a case, the linear transport equation at the steady state can roughly be expressed as $j_y(x)=[\sigma_{xx}(x)+\sigma_{xy}(x)^2\sigma_{xx}(x)^{-1}]E_y$, where x and y are coordinates in the circumference and axis direction, respectively, $j_y(x)$ is the local current density, and E_y is the electric field. This shows, for example, in a high magnetic field, when the Fermi energy is at $\varepsilon=0$, that the conductance is independent of the scattering strength because σ_{xx} given by natural constants independent of the field strength contributes to the conductance.[19] Furthermore, when the scattering is weak and the Fermi energy is at plateau regions of the conductivity σ_{xy}, the conductivity σ_{xx} vanishes. In this case, most of the current is carried by these regions of the nanotube.

A 2D graphite sheet does not exist in nature. One possible candidate may be graphite intercalation compounds of stage 1 having isolated graphite sheets separated from each other by an intercalant layer. However, the interaction between the graphite layer and intercalants alters the band structure considerably. In fact, most intercalation compounds have Fermi surfaces consisting of a three-dimensional sphere (originating from so-called interlayer states) and that of 2D graphite.[36] Therefore, they do not provide a realistic 2D graphite sheet for the measurement of magnetrotransport.

In some graphite systems, weak disorder results in stacking faults, giving rise to a small increase in the interlayer distance. When a special value (0.344 nm) is reached, the stacking of individual graphite layers becomes uncorrelated and the resulting two-dimensional honeycomb structure of uncorrelated graphite layers is called turbostratic graphite.[37,38] This turbostratic graphite may be a candidate for the transport measurement of a 2D graphite.

The recent development in microfabrication technology has enabled fabrication of various artificial structures such as quantum dots, wires, point contacts, etc., at high-mobility semiconductor heterostructures. In particular, an artificial 2D lattice can be fabricated by periodic arrays of antidots and a honeycomb structure is realized by a hexagonal antidot array. Such an artificial antidot lattice can be another promising system where the transport of the 2D graphite can be measured experimentally.

V. SUMMARY

The Hall conductivity of a two-dimensional graphite system has been calculated in a magnetic field within the self-consistent Born approximation. The analytical expressions of the Hall conductivity have been derived in the two cases of dominant short- and long-range scatterers. In the strong-magnetic-field limit, it has been found that the phenomenological relation between $\Delta\sigma_{xy}$ and σ_{xx} holds for the case of

short-range scatterers. The same is true in the long-range case if the difference between τ and τ_{tr} is properly taken into account. In the limit of a weak magnetic field and in the Boltzmann limit the Hall conductivity of quantum transport theory agrees with the Boltzmann result. Numerical calculations have been performed for several typical scattering strength. The Hall conductivity displays the quantum Hall effect when the electron Fermi energy is in low-lying Landau levels and the scattering is relatively weak. On the other hand, when the Fermi energy becomes far away from $\varepsilon=0$, the Hall conductivity in the SCBA tends to the corresponding Boltzmann result.

ACKNOWLEDGMENTS

This work was supported in part by Grants-in-Aid for Scientific Research and for COE Research (12CE2004 ''Control of Electrons by Quantum Dot Structures and Its Application to Advanced Electronics'') from Ministry of Education, Science, Culture, and Sports, Japan. One of the authors (Y.Z.) would like to thank the Ministry for support and acknowledges the National Science Foundation of China (NNSFC) for financial support under Grant Nos. NNSFC69890220 and NNSFC69971012. Y.Z. also wishes to thank T. Yaguchi, Dr. H. Suzuura, Dr. S. Uryu, and other workers in the group for some help. Numerical calculations were performed in part using the facilities of the Supercomputer Center, Institute for Solid State Physics, University of Tokyo.

APPENDIX A: WEAK-FIELD LIMIT OF HALL CONDUCTIVITY

The Hall conductivity must disappear when the magnetic field tends to zero for both cases of short- and long-range scatterers. We give an analytical demonstration of the weak-magnetic-field limit of the Hall conductivity as below.

1. Short-range scatterers

Noting that $\Delta\sigma_{xy}(0)=0$, the Hall conductivity can be written as

$$\sigma_{xy}=\frac{e^2}{\pi^2\hbar}\frac{1}{(\hbar\omega)^2}\int_0^{\varepsilon}2A\,\mathrm{Im}\,\Sigma(\varepsilon')d\varepsilon' + \int_0^{\varepsilon}d\varepsilon' f(\varepsilon')\frac{d}{d\varepsilon'}\Delta\sigma_{xy}(\varepsilon'), \tag{A1}$$

for the case of short-range scatterers. By using the Euler-Maclaurin formula, the self-energy can be expressed as

$$\Sigma=\frac{1}{A}\int\frac{(\varepsilon-\Sigma)dt}{(\varepsilon-\Sigma)^2-t}-\frac{(\hbar\omega)^4}{12A}\frac{1}{(\varepsilon-\Sigma)^3}+\cdots, \tag{A2}$$

where the terms with higher powers than $(\hbar\omega)^4$ have been ignored. We write the dependence of self-energy on $\hbar\omega$ formally as

$$\Sigma=\Sigma_0+\Sigma_1(\hbar\omega)^2+\Sigma_2(\hbar\omega)^4+\cdots. \tag{A3}$$

Then substituting it into Eq. (A2), we have

$$\Sigma_0=\frac{1}{A}\int_0^{\varepsilon_c^2}\frac{(\varepsilon-\Sigma_0)dt}{(\varepsilon-\Sigma_0)^2-t},$$

$$\Sigma_1=0,$$

$$\Sigma_2=-\frac{1}{12(\varepsilon-\Sigma_0)^2[A\varepsilon+2(\varepsilon-\Sigma_0)]}, \tag{A4}$$

where ε_c is a cutoff energy introduced to avoid divergence.

With the above results, the integrands in Eq. (A1) can be expanded as a power series of $(\hbar\omega)^2$. It will be seen that the terms proportional to $(\hbar\omega)^{-2}$ and $(\hbar\omega)^0$ vanish. The remaining terms in the expression of the Hall conductivity are proportional to either $(\hbar\omega)^2$ or higher powers of $(\hbar\omega)^2$, which tend to zero at the weak-magnetic-field limit. Then one comes to the conclusion that the Hall conductivity disappears in the absence of a magnetic field for the case of short-range scatterers.

2. Long-range scatterers

For the case of long-range scatterers, the Hall conductivity is written as

$$\sigma_{xy}=\frac{e^2}{\pi^2\hbar}\frac{1}{(\hbar\omega)^2}\int_0^{\varepsilon}A[\mathrm{Im}\,\Sigma^+ + \mathrm{Im}\,\Sigma^-]d\varepsilon' + \int_0^{\varepsilon}d\varepsilon' f(\varepsilon')\frac{d}{d\varepsilon'}\Delta\sigma_{xy}(\varepsilon'). \tag{A5}$$

By using the Euler-Maclaurin formula, the self-energy for the case of long-range scatterers can be expressed as

$$\Sigma^{\pm}=\frac{1}{A}\int\frac{(\varepsilon-\Sigma^{\mp})dt}{(\varepsilon-\Sigma^+)(\varepsilon-\Sigma^-)-t}\pm\frac{(\hbar\omega)^2}{2A}\frac{1}{\varepsilon-\Sigma^{\pm}} - \frac{(\hbar\omega)^4}{12A}\frac{1}{(\varepsilon-\Sigma^{\pm})^2(\varepsilon-\Sigma^{\mp})}+\cdots. \tag{A6}$$

Expanding the self-energy $\Sigma^{\pm}$ in terms of $(\hbar\omega)^2$ formally as

$$\Sigma^{\pm}=\Sigma_0^{\pm}+\Sigma_1^{\pm}(\hbar\omega)^2+\Sigma_2^{\pm}(\hbar\omega)^4+\cdots, \tag{A7}$$

and substituting it into Eq. (A6), we have

$$\Sigma_0=\frac{1}{A}\int\frac{(\varepsilon-\Sigma_0)dt}{(\varepsilon-\Sigma_0)^2-t},$$

$$\Sigma_1^+=-\Sigma_1^-=\frac{1}{2A(\varepsilon-2\Sigma_0)},$$

$$\Sigma_2^+=\Sigma_2^-=-\frac{1}{4}\frac{1}{A\varepsilon+2(\varepsilon-\Sigma_0)}\left(\frac{1}{3(\varepsilon-\Sigma_0)^2} - \frac{1}{A(\varepsilon-2\Sigma_0)(\varepsilon-\Sigma_0)}+\frac{1}{A^2(\varepsilon-2\Sigma_0)^2}\right). \tag{A8}$$

Following the same procedure as in the case of short-range scatterers, the integrands in Eq. (A5) are expanded as a

power series of $(\hbar\omega)^2$ by using the above result about self-energy $\Sigma^{\pm}$. The expanding of $\Delta\sigma_{xy}(\varepsilon')$ should be started with Eqs. (59)–(64). It will be seen that only the terms proportional to either $(\hbar\omega)^2$ or the higher powers of $(\hbar\omega)^2$ are left in the series, which disappear when the magnetic field tends to zero at the weak-magnetic-field limit. Therefore, the Hall conductivity vanishes in the zero-field limit also for the case of long-range scatterers.

APPENDIX B: BOLTZMANN LIMIT OF HALL CONDUCTIVITY

The Boltzmann limit of the Hall conductivity is derived from the SCBA result in this appendix.

1. Short-range scatterers

In the expression of the Hall conductivity, the first part $-ecn_e/B$ gives a term proportional to $(\hbar\omega)^2$, which is

$$\frac{e^2}{\pi^2\hbar}(\hbar\omega)^2 2A\int_0^{\varepsilon}\mathrm{Im}\Sigma_2(\varepsilon')d\varepsilon', \tag{B1}$$

where Σ_2 is given by Eq. (A4). When $A\gg 1$, except at the extreme vicinity of $\varepsilon'=0$, the self-energy $\Sigma_0(\varepsilon')\approx -\pi i|\varepsilon'|/A$ is much smaller than ε', which causes Σ_2 to decrease very rapidly for sufficiently large ε' ($\Sigma_2\propto\varepsilon'^{-3}$). Further, due to the symmetry of $\mathrm{Im}\,\Sigma_2(\varepsilon')$ with respect to ε', the above integral is approximated by

$$\mathrm{Im}\int_{-\varepsilon}^{\varepsilon}\Sigma_2(\varepsilon')d\varepsilon'\approx\mathrm{Im}\int_{-\infty}^{\infty}\Sigma_2(\varepsilon')d\varepsilon'=0, \tag{B2}$$

where the analyticity of $\Sigma_2(\varepsilon')$ in the upper complex plane has been used.

Only the following term remains when $\Delta\sigma_{xy}(\varepsilon)$ is expanded in terms of $(\hbar\omega)^2$ and all other terms are much smaller:

$$\Delta\sigma_{xy}(\varepsilon)=\frac{e^2}{\pi^2\hbar}2\Gamma_0^2(\hbar\omega)^2 \times\mathrm{Im}\int\frac{2[|\varepsilon-\Sigma_0|^2+t]|\varepsilon-\Sigma_0|^2dt}{[(\varepsilon-\Sigma_0)^2-t][(\varepsilon-\Sigma_0^*)^2-t]^4}. \tag{B3}$$

In the Boltzmann limit, the above becomes

$$\Delta\sigma_{xy}(\varepsilon)=-\mathrm{sgn}(\varepsilon)\frac{e^2}{\pi^2\hbar}\frac{\pi(\hbar\omega)^2}{16\Gamma_0^2}=-\omega_c\tau\sigma_0, \tag{B4}$$

in agreement with the Boltzmann result.

2. Long-range scatterers

There are three terms of Σ_2 in Eq. (A8) for the case of long-range scatterers. However, it can be justified that the contributions of them to the Hall conductivity can be ignored with the same measure of the case of short-range scatterers. Then we need only consider the terms proportional to $(\hbar\omega)^2$ in $\Delta\sigma_{xy}(\varepsilon)$. The contribution from σ_a can be ignored and the following terms should be retained when expanding $\varphi(\varepsilon-i0,\varepsilon+i0)$ in terms of $(\hbar\omega)^2$:

$$\varphi(\varepsilon-i0,\varepsilon+i0)=\frac{1}{2}-i\frac{\pi\mathrm{sgn}(\varepsilon)(\hbar\omega)^2}{2^3A[\mathrm{Im}\Sigma_0(\varepsilon)]^2}\left[1+i\frac{(\hbar\omega)^2}{2^2\varepsilon\,\mathrm{Im}\,\Sigma_0(\varepsilon)}-\frac{(\hbar\omega)^4}{2^4\varepsilon^2[\mathrm{Im}\,\Sigma_0(\varepsilon)]^2}+\cdots\right]. \tag{B5}$$

Substituting the above into the expression of σ_b, we obtain the Hall conductivity as

$$\Delta\sigma_{xy}(\varepsilon)=-\mathrm{sgn}(\varepsilon)\frac{e^2}{\pi^2\hbar}\frac{\pi(\hbar\omega)^2}{4\Gamma_0^2}=-\omega_c\tau_{\mathrm{tr}}\sigma_0, \tag{B6}$$

in agreement with the Boltzmann result.

*Permanent address: Department of Physics, Jilin University, Changchun 130023, China.

[1] S. Iijima, Nature (London) **354**, 56 (1991).
[2] S.N. Song, X.K. Wang, R.P.H. Chang, and J.B. Ketterson, Phys. Rev. Lett. **72**, 697 (1994).
[3] L. Langer, V. Bayot, E. Grive, J.P. Issi, J.P. Heremans, G.H. Olk, L. Stockman, C. Van Haesendonck, and Y. Brunseraede, Phys. Rev. Lett. **76**, 479 (1996).
[4] S.J. Tans, M.H. Devoret, H.J. Dai, A. Thess, R.E. Smalley, L.J. Geerligs, and C. Dekker, Nature (London) **386**, 474 (1997).
[5] P.L. McEuen, M. Bockrath, D.H. Cobden, Y.-G. Yoon, and S.G. Louie, Phys. Rev. Lett. **83**, 5098 (1999).
[6] R. Saito, G. Dresselhaus, and M.S. Dresselhaus, Phys. Rev. B **53**, 2044 (1996).
[7] Y. Miyamoto, S.G. Louie, and M.L. Cohen, Phys. Rev. Lett. **76**, 2121 (1996).
[8] L. Chico, L.X. Benedict, S.G. Louie, and M.L. Cohen, Phys. Rev. B **54**, 2600 (1996).
[9] T. Seri and T. Ando, J. Phys. Soc. Jpn. **66**, 169 (1997).
[10] T. Ando and T. Seri, J. Phys. Soc. Jpn. **66**, 3558 (1997).
[11] T. Ando and T. Nakanishi, J. Phys. Soc. Jpn. **67**, 1704 (1998).
[12] T. Ando, T. Nakanishi, and R. Saito, J. Phys. Soc. Jpn. **67**, 2857 (1998).
[13] M. Igami, T. Nakanishi, and T. Ando, J. Phys. Soc. Jpn. **68**, 716 (1999).
[14] M. Igami, T. Nakanishi, and T. Ando, J. Phys. Soc. Jpn. **68**, 3146 (1999).
[15] T. Ando, T. Nakanishi, and M. Igami, J. Phys. Soc. Jpn. **68**, 3994 (1999).
[16] H.J. Choi and J. Ihm, Solid State Commun. **111**, 385 (1999).
[17] H.J. Choi, J. Ihm, S.G. Louie, and M.L. Cohen, Phys. Rev. Lett. **84**, 2917 (2000).
[18] For a review, see, for example, T. Ando, Semicond. Sci. Technol. **15**, R13 (2000).
[19] N.H. Shon and T. Ando, J. Phys. Soc. Jpn. **67**, 2421 (1998).
[20] T. Ando and Y. Uemura, J. Phys. Soc. Jpn. **36**, 959 (1974).
[21] J.W. McClure, Phys. Rev. **104**, 666 (1956).
[22] H.J. Fischbeck, Phys. Status Solidi **38**, 11 (1970).

[23] M. Igami, S. Okada, and K. Nakada, Synth. Met. **121**, 1233 (2001).
[24] H.A. Mizes and J.S. Foster, Science **224**, 559 (1989).
[25] M. Endo, T. Hayashi, S. Hong, T. Enoki, and M.S. Dresselhaus, J. Appl. Phys. **90**, 5670 (2001).
[26] R. Kubo, J. Phys. Soc. Jpn. **12**, 570 (1957).
[27] R. Kubo, H. Hasegawa, and N. Hashitsume, J. Phys. Soc. Jpn. **14**, 56 (1959).
[28] R. Kubo, S.J. Miyake, and N. Hashitsume, in *Solid State Physics*, edited by F. Seitz and D. Turnbull (Academic Press, New York, 1965), Vol. 17, p. 269.
[29] H. Shiba, K. Kanda, H. Hasegawa, and H. Fukuyama, J. Phys. Soc. Jpn. **30**, 972 (1971).
[30] T. Ando, Y. Matsumoto, and Y. Uemura, J. Phys. Soc. Jpn. **39**, 279 (1975).
[31] T. Ando, J. Phys. Soc. Jpn. **37**, 1233 (1974).
[32] B.L. Al'tshuler, A.G. Aronov, and B.Z. Spivak, Pis'ma Zh. Éksp. Teor. Fiz. **33**, 101 (1981) [JETP Lett. **33**, 94 (1981)].
[33] H. Ajiki and T. Ando, J. Phys. Soc. Jpn. **62**, 1255 (1993).
[34] A. Bachtold, C. Strunk, J.P. Salvetat, J.M. Bonard, L. Forró, T. Nussbaumer, and C. Schönenberger, Nature (London) **397**, 673 (1999).
[35] A. Fujiwara, K. Tomiyama, H. Suematsu, M. Yumura, and K. Uchida, Phys. Rev. B **60**, 13 492 (1999).
[36] H. Zabei and S. A. Solin, *Graphite Intercalation Compounds II* (Springer-Verlag, Berlin, 1992).
[37] J. Maire and J. Méring (unpublished).
[38] M. S. Dresselhaus, G. Dresselhaus, K. Sugihara, I. L. Spain, and H. A. Goldberg, *Graphite Fibers and Filaments*, Vol. 5 of *Springer Series in Materials Science* (Springer-Verlag, Berlin, 1988).